Solid State Ionics 301 (2017) 86–94

Contents lists available at ScienceDirect

Solid State Ionics

journal homepage: www.elsevier.com/locate/ssi

Proton and cesium conductivity in perfluorosulfonate ionomers at low and high relative humidity

Bruno R. Matos [a,*], Jaqueline S. da Silva [a], Elisabete I. Santiago [a], Duclerc F. Parra [a], Danilo J. Carastan [b], Daniel Z. de Florio [b], Heber E. Andrada [c], Alejo C. Carreras [c,d], Fabio C. Fonseca [a]

[a] Instituto de Pesquisas Energéticas e Nucleares, IPEN-CNEN, São Paulo, SP 05508000, Brazil
[b] Universidade Federal do ABC, UFABC, Santo André, SP 09219170, Brazil
[c] Facultad de Matemática, Astronomía y Física, Universidad Nacional de Córdoba, Medina Allende s/n, 5016 Córdoba, Argentina
[d] Instituto de Física Enrique Gaviola (IFEG), CONICET, Argentina

ARTICLE INFO

Article history:
Received 17 November 2015
Received in revised form 13 January 2017
Accepted 23 January 2017
Available online xxxx

Keywords:
Membranes
Charge transport
Electrochemistry
Ionomers

ABSTRACT

Nafion exhibits one of the highest proton conductivity at room temperature and it is the standard electrolyte of proton exchange membrane fuel cells (PEMFC). However, the temperature dependence of ionic conductivity of Nation is highly dependent on the measuring conditions and it is still a matter of debate. In the present study, detailed dielectric spectroscopy (DS) measurements in both dry (under N_2 flow) and water-saturated conditions were carried out in a broad range of temperature and frequency. Such DS results were correlated to differential scanning calorimetry (DSC) and dynamic mechanical analysis (DMA) data taken in similar conditions. The main results revealed that in samples conditioned in N_2 flow (*RH* ~0%) the transport of both proton and cesium ions is coordinated with the dynamics of Nafion relaxations. In hydrated Nafion (proton form), conductivity measurements at different frequencies revealed two regimes: one at high-frequency, in which the Vogel-Tamman-Fulcher (VTF) law indicates a close relation between the polymer glass transition temperature T_g; and, a second one at low frequency, bearing great similarity to the transport observed in nearly dry samples. The reported experimental results contribute to disentangle the intricate transport properties of Nafion.

1. Introduction

Nafion (Dupont) is a leading polymer from a family of perfluorosulfonate ionomer membranes that are produced under different trademarks (3M, Dow, Flemion, Aciplex, Hyflon) and possesses one of the highest proton conductivity among solid proton conductors [1]. Recently, the relationship between the proton conductivity and the relaxation dynamics at a high temperature (HT) range (~80–140 °C) is pursued in order to identify the underlying mechanisms responsible for the transport properties of Nafion in HT polymer electrolyte fuel cells (PEFC). At this temperature range, polymer thermal transitions take place and can affect significantly the performance of PEFC [1,2].

In order to advance the understanding of the relation between microstructure and electric properties in Nafion at HT, the dependence of mechanical and dielectric relaxations upon water content must be taken into account [2,3,4]. It has been generally accepted that the water uptake capacity of ionomer samples is dependent on the flexibility of polymer chains, which allows polymer expansion upon water sorption. However, the water sorption of ionomers increases both the proton dissociation and the flexibility of the polymer chains, both of which increase the proton conductivity of Nafion. Such effect makes the determination of the exact contribution to the proton conductivity of ionomers a hard task [2,3,4]. In this context, mechanical/dielectric relaxations studies dedicated to the role played by the water sorption on the flexibility and conductivity of ionomers are scarce [5,6,7,8].

Furthermore, several authors identified anisotropic water transport in Nafion at *RH* < 100% [9], suggesting that the proton conduction is preferred along one of the directions of the ionomer main chains. Therefore, the investigation of the proton conduction properties of Nafion films conditioned at *RH* ~0%, when the proton charges are mostly coordinated with the polymer chains, must be the preliminary characterization for understanding the dependence of the proton conductivity on the motion of the polymer chains. Nonetheless, the study of the conductivity of Nafion at *RH* ~0% is useful for eliminating the contribution of the water and for determining the role of the polymer relaxations to the transport properties.

A considerable data set of the proton conductivity of Nafion has been published [1–15]. However, most of the reported data was collected in a rather limited range of temperature and relative humidity. Conductivity measurements of Nafion at *RH* ~0% and the correspondence between thermal/mechanical/dielectric properties and ion conductivity at such

* Corresponding author.
E-mail address: brmatos@usp.br (B.R. Matos).

http://dx.doi.org/10.1016/j.ssi.2017.01.019
0167-2738/

condition are rarely found [5,6,8,16]. Arrhenius plots of Nafion proton conductivity at *RH* ~0% were previously reported to be composed of two distinct regimes [6,7]. At low temperatures (*T* ~20–90 °C) Arrhenius-like temperature dependence is usually reported, whereas at higher temperatures (*T* > 90 °C) a deviation from the Arrhenius behavior has been observed [6,7]. The non-Arrhenius behavior of the proton conductivity, identified as a conductivity upturn at *T* > 90 °C was fitted with the Vogel-Tamman-Fulcher (VTF) equation and related to the cooperative motion of the main ionomer chains with the charge transport [6,7,16]. Although this result is in accordance with the VTF empirical law, such measurements of the proton conductivity of Nafion at *RH* ~0% have been limited to a limited temperature range (*T* ~20–120 °C) [7]. Dielectric spectroscopy (DS) studies have been performed at anhydrous conditions in a more extended *T*-range (−155 °C to +155 °C) for perfluorosulfonate ionomer membranes such as 3 M membranes, Nafion and Nafion containing ionic liquids [6,8,16]. Such DS data confirmed the presence of non-Arrhenius behavior, which was considered to be a result of the VTF-temperature dependence [8,16]. The VTF behavior was also observed for Nafion β-relaxation at anhydrous condition and at low *RH* (the ratio $H_2O/SO_3H = 6$) [17], thereby confirming the cooperative transport between charge and segmental chain motions.

The intricate relationship between the relaxation dynamics and the proton conduction properties of nearly dry perfluorosulfonate ionomers has its counterpart in the hydrated state. Recently, it was shown that the temperature dependence of proton conduction of hydrated Nafion, measured at constant *RH* = 100%, is similar to the one observed at *RH* ~0%: an Arrhenius regime in the *T* ~30–90 °C range and a non-Arrhenius upturn of proton conductivity for *T* > 90 °C, which could be also fit with the VTF equation [15,16]. More recent studies, performed at low water content (~3–6 water molecules per SO_3H) and at constant water partial pressure, evidenced basically two regimes in the proton conductivity of Nafion: an Arrhenius portion of the curve up to ~80 °C, followed by a decrease of proton conductivity of the ionomer at *T* > 120 °C [2]. Such results suggest that the conductivity of Nafion at constant water partial pressure is strongly dependent on the sample water content. The proton conductivity of Nafion at constant water partial pressure decreases for *T* > 100 °C due to a dramatic loss of water from the sample [2,18], whereas the proton conductivity and the water content measured in a closed system (*RH* ~100%) increase in the temperature interval 40–180 °C [11,15]. Thus, the conductivity upturn at high *T* can be attributed to the increasing water uptake, while the chain dynamics plays a minor role in the charge transport.

Moreover, it is interesting to note that the temperature dependence of the proton conductivity of Nafion displays irreversibility when consecutive measurements are carried out [15]. Particularly, the non-Arrhenius portion of the conductivity curve is absent in the second heating (*RH* = 100%). On the other hand, the polymer glass transition (T_g) is not expected to change significantly upon successive heatings [19]. Therefore, the irreversibility of the proton conductivity puts in doubt the validity of the VTF law at high *T*, as the VTF behavior is dependent on the polymer T_g.

Previous broadband DS studies suggested that the proton conductivity of Nafion was modulated by the motion of main and side chains [6,8]. However, the interpretation of Nafion electric/dielectric spectra is under intense debate, as different mechanisms for the same observed dielectric relaxations were given [5–8,11,20–21]. From the earliest reports on the dielectric spectroscopy of Nafion up to the present days, the dielectric relaxations were attributed to the polymer relaxations due to the correspondence with dynamic mechanical analysis (DMA) and differential scanning calorimetry (DSC) [5–6,11,20–21]. Nonetheless, new interpretations of the dielectric spectra of Nafion emerged, which assigned the dielectric relaxations observed to electrode polarization phenomena [7,16]. Recently, the interpretation of the Nafion's dielectric spectra is being revisited [11,20,22] in which new findings obtained by time-dependent SAXS coupled with *dc* potential, and electrode polarization characterizations suggested that the dielectric relaxations must be attributed to the polymer relaxations [22]. Nevertheless, such attributions remain controversial and different approaches are confronted [16,20,22].

In this context, the mechanism underlying the temperature dependence of proton conductivity is an open problem and no consensus has been reached concerning the role played by both the water and the relaxation dynamics on the transport properties of perfluorosulfonate ionomer membranes [8,24].

In this scenario, the investigation of the relationship between cesium conductivity-glass transition is opportune, as the glass transition temperature of Nafion in the cesium form is ~130 °C, which is ~150 °C higher than the glass transition of Nafion in the protonic form [8,19].

Thus, the present study investigates the ion conductivity in a wide range of frequency, temperature, and relative humidity of Nafion, in both the proton and cesium forms, to investigate the role played by: *i)* the water content; and *ii)* the dynamics of Nafion relaxations. A good correspondence between DMA, DSC and DS adds evidences that the electric/dielectric spectra of Nafion display contributions from the bulk polymer. Moreover, the matching between the transport properties at *RH* ~0 and 100% shows that even at fully hydrated condition, the ion conductivity of Nafion is dependent on the mobility of the polymer chains.

2. Experimental

Commercial Nafion 115 membranes ($EW = 1100$ g Eq^{-1}) were obtained from DuPont. The membranes were pre-treated by standard cleaning and activation protocols [15]. Hydrated samples (in the protonic form) were characterized without previous thermal treatment to avoid morphological changes. To obtain samples in the cesium forms (Nafion-Cs^+), Nafion acid (Nafion-H^+) films were immersed in cesium chloride solutions (1 mol L^{-1}) at 80 °C for 1 h. This step was repeated three times to assure a higher degree of ionic conversion. Then, samples were copiously washed with deionized water to remove the excess of reagents.

Small angle X-ray scattering (SAXS) experiments were carried out using synchrotron radiation at the SAXS beamline of the Brazilian National Synchrotron Light Laboratory (LNLS/project number 18801). Experiments were conducted with an incident wavelength $\lambda = 1.488$ Å in the range of the scattering vector q ~0.02–0.35 $Å^{-1}$ ($q = 4\pi \sin\theta/\lambda$, being 2θ the scattering angle). Scattering patterns were collected with MarCCD detector and the intensity curves were corrected for parasitic scattering, integral intensity, and sample absorption. For in situ heated SAXS measurements as a function of temperature, N115 samples were positioned in a special sample-holder, consisting of a metallic clamps coupled with a resistive heating. The sample-holder has a ~3 mm window for the X-ray beam and the measurements were performed in the 40–160 °C *T*-range under N_2 flow.

Thermogravimetric (TGA) measurements (Setaram-LabSys) were carried out in the 25–250 °C temperature range at a heating rate of 5 °C/min under nitrogen flow. This setting was used to measure the mass loss of previously vacuum dried samples at 25 °C for 1 h.

Dielectric spectroscopy (DS) measurements were performed on samples using a specially designed airtight sample holder. Such a device allows electrical measurements (through-plane) controlling both the temperature (from room temperature up to *T* ~ 200 °C) and the relative humidity (*RH*, from ~3 to 100%) [1]. Temperature controllers connected to band heaters placed externally around the cylindrical sealed chambers are monitored by thermocouples (type K) inserted inside its metallic walls. Nafion samples were sandwiched with carbon cloths between stainless steel spring-load contact terminals, insulated from the chamber walls. The carbon cloth electrodes are treated in nitric acid solution and excess deionized water to remove impurities ensuring that these electrodes can be considered blocking electrodes. Before studying the electric properties of the ionomer samples, several experiments were

performed to ensure that the bulk properties of the sample under investigation are properly accessed. Some of the checked parameters were: different electrode materials (platinum, carbon cloth, and gold), the area of the electrodes was varied (0.785 cm^2, 5 cm^2, and 25 cm^2), different electrode distances by using different membrane thicknesses [24], short-circuited sample-holder correction, and comparison between through-plane and in-plane conductivity measurements. In-plane measurements were carried out in a commercial sample holder (FuelCon® TrueXessory-PCM). Such series of experiments are important to separate contributions arising from the measuring apparatus (sample-holder, connection cables and the impedance analyzer) and electrodes. The ionic conductivity measurements of dry samples was carried out by positioning the sample in the sample-holder and allowing the system to reach equilibrium at 30 °C under N_2 flow for 24 h. Two successive heatings were performed for each sample.

A Solartron 1260 frequency response analyzer was used in the frequency (f) range of 4 mHz to 3 MHz applying an *ac* amplitude of 100 mV. The complex conductivity ($\sigma^* = 2\pi f\varepsilon_0\varepsilon^*$) and dielectric permittivity ($\varepsilon^* = \varepsilon' + i\varepsilon''$) representations were used throughout this study, in which the dielectric loss ($\varepsilon''(f)$) was obtained from:

$$\varepsilon''(f) = -\frac{dcos(\theta(f))}{2\pi f\varepsilon_0 S|Z(f)|}, \quad (1)$$

where ε' and ε'' are the real and imaginary parts of the dielectric permittivity; ε_0 is the vacuum permittivity (~8.854×10^{-14} F cm^{-1}); S is the electrode active area, d is the thickness of the membrane; $|Z|$ and θ are the modulus and phase angle of impedance. The high frequency conductivities of dry and hydrated Nafion were determined via intercept with the Z′ axis of the impedance semicircle at $f \sim 10^2$ Hz and $f \sim 10^6$ Hz, respectively. The low frequency conductivity was obtained for hydrated samples at $f < 10^6$ Hz using the relation: $\sigma' = 2\pi f\varepsilon_0\varepsilon''$ [15]. Conductivity measurements were performed in duplicates. The high and low frequency components of the ionic conductivity are referred to as high-f and low-f conductivities throughout the text.

Differential scanning calorimetry (DSC) and dynamic mechanical analysis (DMA) were performed on dry Nafion under nitrogen flow in two successive heatings. The DSC tests were performed from −50 to 250 °C at a heating rate of 20 °C min^{-1} under nitrogen flow in two successive heatings. A fast cooling rate (50 °C min^{-1}) was used between the successive heatings.

Dynamic mechanical analysis (DMA) was carried out under nitrogen flow in a TA Instruments® DMA Q800 in tensile mode. Rectangular Nafion samples (15 × 6 mm^2) were cut and tested in the machine direction with a heating rate of 3 °C min^{-1}, amplitude of 4 μm and oscillation frequency of 1 Hz.

3. Results and discussion

3.1. Relationship between proton conductivity and relaxation for dry Nafion

Under dry N_2 atmosphere (*RH* ~0%), the protonic charges and residual water molecules are mostly coordinated with the polymer chains. The study of the effect of the polymer relaxations on the proton conductivity of samples conditioned at *RH* ~0% is useful because all protonic charges are electrostatically attached to the end of the polymer side chains. In this condition, the ionic conductivity is expected to be coupled to the chain dynamics [25]. However, controlling residual water in the polymer structure is a crucial factor to ensure the reproducibility of such proton conductivity measurements. Moreover, a significant amount of free water molecules is readily reabsorbed when the sample is cooled down to room temperature. Previous studies evidenced the presence of free and coordinated water molecules up to $T \sim 200$ °C in Nafion-H^+ [21,26]. In order to separate contributions arising from the absorbed water, the mechanical/dielectric analysis and the conductivity measurements were performed in two successive heatings and under N_2 flow to ensure that most of the water molecules was removed. Such a procedure is important for separating contributions of chain dynamics from absorbed water on the conductivity.

Thus, prior to conductivity measurements a careful analysis was carried out to evaluate both the amount of water and possible modifications of ionomer structure due to high temperature annealing in dry conditions. Fig. 1 shows the TGA (Fig. 1a) and SAXS (Fig. 1b) plots of vacuum dried Nafion under N_2 flow.

The TGA curve (Fig. 1a) shows the weight loss related to water removal of previously vacuum dried Nafion. Less than 1% of residual water is absorbed, a value which corresponds to ~0.5 water molecules per sulfonic acid groups. Such low H_2O/SO_3H ratio is in good agreement with previous values estimated by NMR ($H_2O/SO_3H \sim 1$) and FTIR for vacuum dried samples [27,28]. In order to evaluate possible structure modifications of Nafion upon heating, Fig. 1b shows the SAXS plots for N115 at 80 and 160 °C performed in two successive heatings.

Usually, SAXS patterns of nearly dry Nafion membranes display two scattering maxima centered at $q = 1.9$ nm^{-1} (ionomer peak) and at $q = 0.5$ nm^{-1} (matrix peak) [2]. The membrane heating leads to the broadening and reduction of the ionomer peak intensity, whereas the

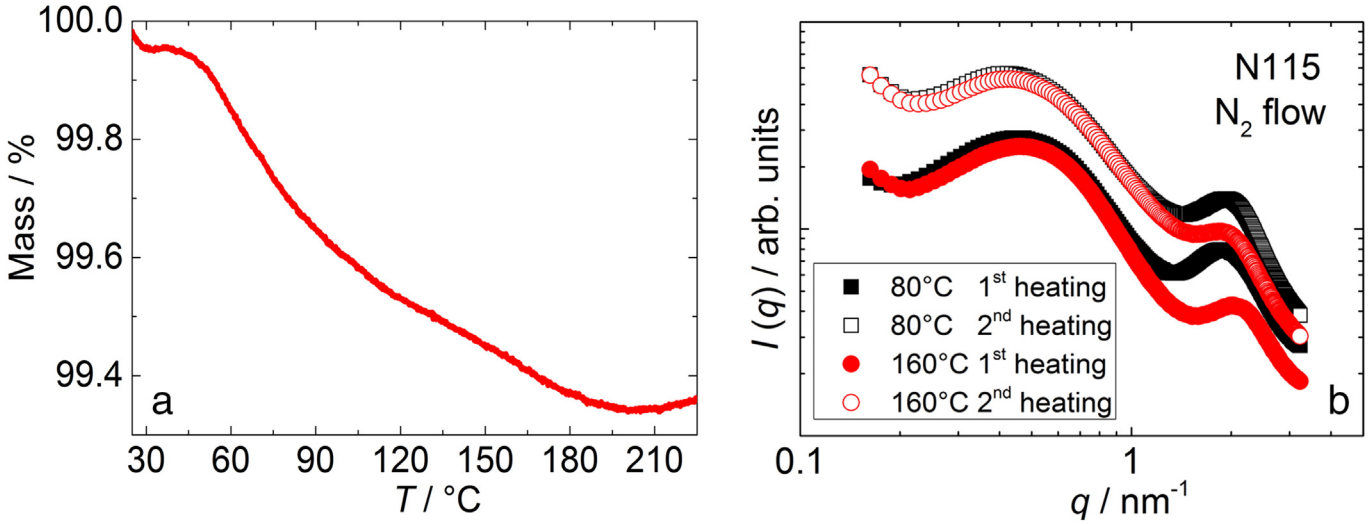

Fig. 1. (a) TGA curves under N_2 flow for previously dried Nafion sample; (b) SAXS plots of Nafion 115 at different temperatures measured during two successive heatings under N_2 flow. The curves for second heatings were displaced vertically, as indicated by the arrow.

Table 1
Ionomer peak to matrix peak ratio at different temperatures.

Condition	Ionomer/matrix peak relative intensity		
	40 °C	80 °C	160 °C
1st heating	0.37	0.29	0.18
2nd heating	–	0.25	0.16

shape and intensity of the matrix peak remains nearly constant. The nearly constant position of the ionomer peak ($q \approx 1.9\ nm^{-1}$) and the small differences in the water loss (<1%) suggest that the changes of the ionomer peak may be associated with morphology transitions within the ionic phase for $T > 80$ °C. Such feature indicates that the changes of the conduction properties of Nafion at high T are mostly associated with the ionic domains rather than changes of the polymer crystallinity and water content. Table 1 shows relative intensity of the ionomer peak with respect to the matrix peak as the temperature increases in the first and second heatings.

For the first heating, it can be observed that the relative intensity of the ionomer peak decreases with increasing temperature. Such reduction of the ionomer peak intensity is irreversible as the original intensity is not recovered in the second heating. Thus, SAXS plots indicate a lower degree of ordering of the nanophase-separated structure of Nafion.

The coupling between the proton conductivity and the relaxation dynamics can be evaluated by comparing the temperature dependence of both the σ and the α-transition. The α-transition can be studied by dielectric spectroscopy (DS), dynamic mechanical analysis (DMA) and differential scanning calorimetry (DSC). Thus, the α-transition was carefully investigated by such techniques in the same experimental conditions, i.e., under N_2 flow and in two consecutive heatings. The DS, DSC and DMA measurements of Nafion as a function of temperature are shown in Fig. 2a, b and c, respectively.

The DS measurements shown in Fig. 2a evidenced the α-relaxation peak centered at $T \sim 130$ °C in the dielectric loss curve. In the second heating the α-transition is attenuated with respect to the first DS measurement and the peak is shifted to $T \sim 150$ °C. Such a feature can be related to irreversible changes in the ionomer morphology upon annealing, as identified by SAXS (Fig.1b) [11,29]. Nevertheless, the relaxation is evident and it occurs in a similar temperature range in both measurements.

The DMA measurements (Fig. 2b) show that Nafion α-relaxation is characterized by an intense dissipation loss occurring at $T \sim 110$ °C in the tan δ plots [19]. In the second heating a reduction of the dissipation factor is observed in close resemblance with the second heating measurement probed by DS (Fig. 2a).

The DSC curves (Fig. 2c) exhibit an endothermic minimum in the first heating centered at $T \sim 150$ °C. However, in the second DSC run such a peak is practically absent. The origin of the DSC endothermic minimum has been associated with different features since it is coincident with different processes observed in the same temperature range such as the α-transition, the ionomer crystallization temperature, and significant loss of water [11,19,30]. However, the low water loss observed by TGA and the morphological changes of the ionic phase indicated by SAXS data suggests that thermal events observed by DSC and DMA must be predominantly assigned to α-transition, which is Nafion thermal transition associated with the weakening of the electrostatic interactions among sulfonic groups.

It is important to note that there is a good agreement between the DSC, DS, and DMA analyses in the first and second heatings. All techniques revealed an attenuation of the thermal event in the second heating in 60–180 °C T-range indicating that they reflect the same phenomena. Such behavior suggests that the DSC endothermic event in dry atmosphere can be linked to α-relaxation, but not to a true glass transition, which should be observed in successive measurements. The lack of correspondence of α-relaxation with a second glass transition in Nafion is in accordance with previous reports [8,19]. The attenuation of the α-

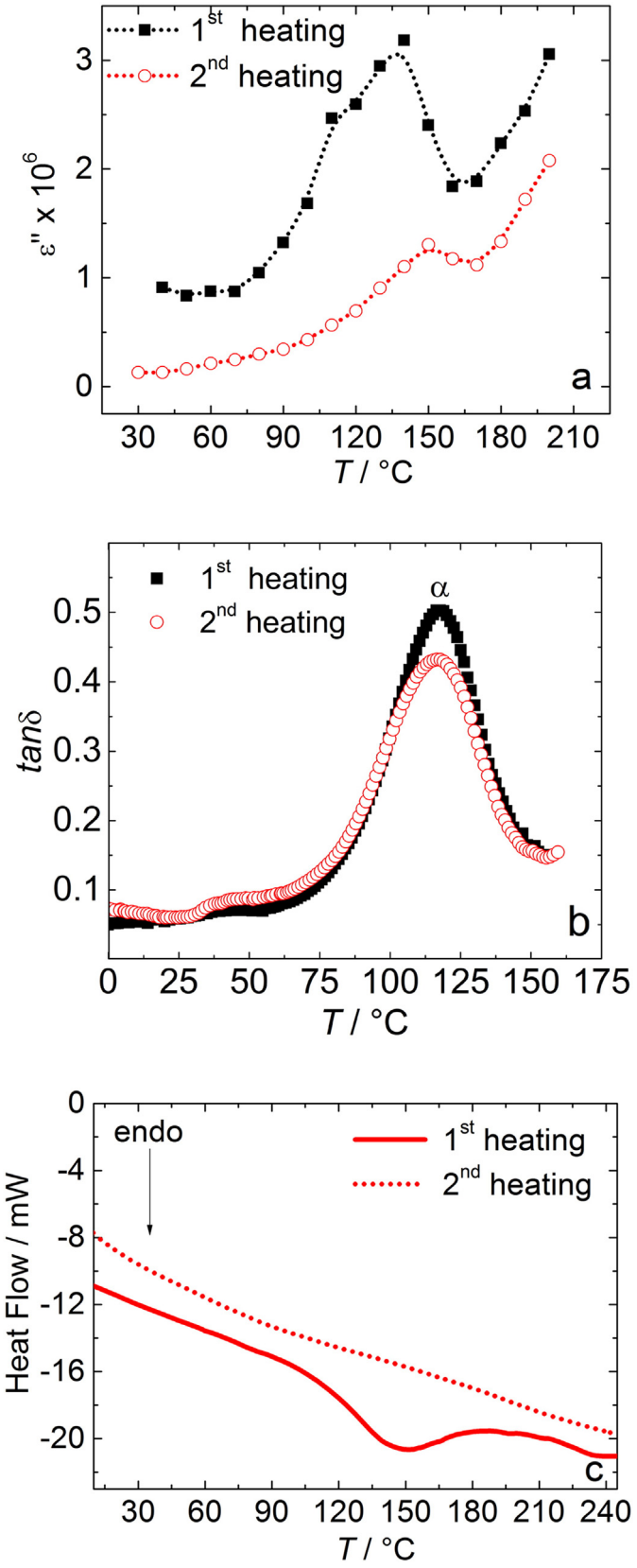

Fig. 2. DS (a), DMA (b) and DSC (c) measurements as a function of temperature in two successive heatings for dry Nafion under N_2 flow. The DS and DMA measurements were both obtained at $f \sim 10^0$ Hz.

relaxation is possibly associated with irreversible morphology changes upon heating the ionomer, possibly due to the restructuring of the electrostatic interactions among sulfonic acid groups at high *T*. However, according to previous thermogravimetric studies such changes are not associated with the irreversible thermal degradation of the polymer chains, which were observed to be relevant in a higher temperature range ($T > 280$ °C) [26].

The α-transition of perfluorosulfonate ionomer films was attributed to the long-range motion of Nafion main and side chains due to the weakening of the electrostatic interactions among sulfonic acid groups [8,19]. Such long-range motion of Nafion chains can affect the proton conductivity in the same temperature range. Fig. 3 shows impedance spectroscopy data for Nafion under N_2 flow in two successive heatings.

Fig. 3 shows the Nyquist plot at $T = 50$ °C (a) and Arrhenius plots for proton conduction in Nafion (b) measured in two successive heatings under N_2 atmosphere. In the Nyquist plot of the first heating (Fig. 3a), it can be observed a high-frequency semicircle with ~0.3×10^5 Ω diameter and a spike at low frequencies ($f < 10^2$ Hz). In the second heating a pronounced increase of the high frequency semicircle reflects an increase of the electrical resistance, along with a well-defined component at low frequency. At $f < 10^2$ Hz, in the second heating a low frequency component of the impedance diagram is observed as a depressed semicircle.

In the first heating (Fig. 3b), an Arrhenius-like temperature dependence of the proton conductivity (obtained at $f \sim 10^2$ Hz) can be observed in the T ~40–70 °C range with activation energy of E_a ~0.07 eV. Such a charge transport process can be assigned to the proton conductivity in bulk free water molecules in the sample via the Grotthuss mechanism (structural diffusion). In the second heating, in the T ~40–70 °C range, the proton conductivity possibly occurs via structural diffusion along the coordinated water molecules. However, due to the coordination of the proton with the polymer chains the charge transport is modulated by the motion of the polymer chains.

Nevertheless, the striking result in Fig. 3 is the temperature dependence of ionic conductivity at higher measuring temperatures ($70 < T < 200$ °C). For $T > 70$ °C both first and second measurements exhibit similar temperature dependence. The proton conductivity increases with increasing temperature, reaching a maximum at T ~120 °C, in agreement with data shown in Fig. 2. Further increasing temperature ($T > 120$ °C) results in a decrease of proton conductivity with a local minimum at T ~170 °C. For $T > 170$ °C the increase of the proton conductivity is resumed up to the highest measured temperature ($T = 200$ °C). Such unusual temperature dependence was reproduced in the two measurements indicating that no significant thermal degradation occurred upon annealing and only uncoordinated water molecules were removed [26,31]. In fact, previous thermal analyses showed that under N_2 the first irreversible thermal event is the loss of sulfonic acid groups, occurring at T ~300 °C [31]. The deviation of the ionic conductivity from the Arrhenius behavior was previously observed for poly(3-alkylthiophene) [32]. In such polymer, the conductivity followed the same temperature dependence of the α-transition, similarly to the behavior observed for Nafion. Such feature was related to the coupling between the electric transport and thermal motions of both the side and main chains [32]. It is worth noting that conductivity maximum (T ~120 °C) and the α-transition as observed in the DMA data (Fig. 2b) occur at similar temperature, supporting that the proton conductivity is a result of the coupling between the ion transport and the dynamics of chains. Thus, the deviation from the thermally activated behavior for $T > 120$ °C suggests that the proton conductivity of Nafion is possibly modulated by the α-transition.

Measurements of samples at *RH* ~0% displayed in Figs. 2 and 3 suggest that temperature dependence of the protonic transport along the side chain-attached sulfonic groups via ion-hopping is modulated by motion of Nafion chains. In addition, as can be clearly observed in Fig. 3, the proton conduction does not follow the VTF law at $T > 70$ °C. The absence of the VTF behavior indicates that the glass transition (occurring at T_g ~− 20 °C) plays a minor role in the transport properties of nearly dry samples. Moreover, the combined data of Figs. 2 and 3 are in agreement with previous reports that showed that the α-relaxation cannot be considered as a true a glass transition.

3.2. Relationship between cesium conductivity and relaxation for Nafion

In order to advance on the study of the relationship between the ion conductivity and relaxation dynamics, DSC, DS and conductivity measurements were performed at *RH* ~0% on Nafion samples neutralized with cesium counterions (Nafion-Cs^+). It has been shown by DMA and DSC that the ion exchange from Nafion-H^+ to Nafion-Cs^+ increases the temperature of glass transition from −20 °C to ~130 °C, respectively [19,21]. Thus, such a pronounced difference of T_g can be helpful to separate contributions arising from the α and glass transition to the ion conductivity of Nafion. Fig. 4 shows DSC curve (Fig. 4a), the high-frequency conductivity for Nafion-Cs^+ for both *RH* = 10% and under N_2 flow the temperature dependence of the β-relaxation frequency (Fig. 4b), and the temperature dependence of the β-relaxation frequency (Fig. 4c).

In accordance with previous reports, the DSC curve of Nafion-Cs^+ (Fig. 4a) exhibits a stepwise decay of the heat flow at T ~112 °C, which was assigned to the glass transition temperature [19]. It is worth noting that the replacement of the protons for cesium counterions increases both the glass transition (from −20 °C to 130 °C) and the α-transition temperature from 110 °C (H^+) to 240 °C (Cs^+) [19]. Such a transition shift is an interesting advantage for studying Nafion-

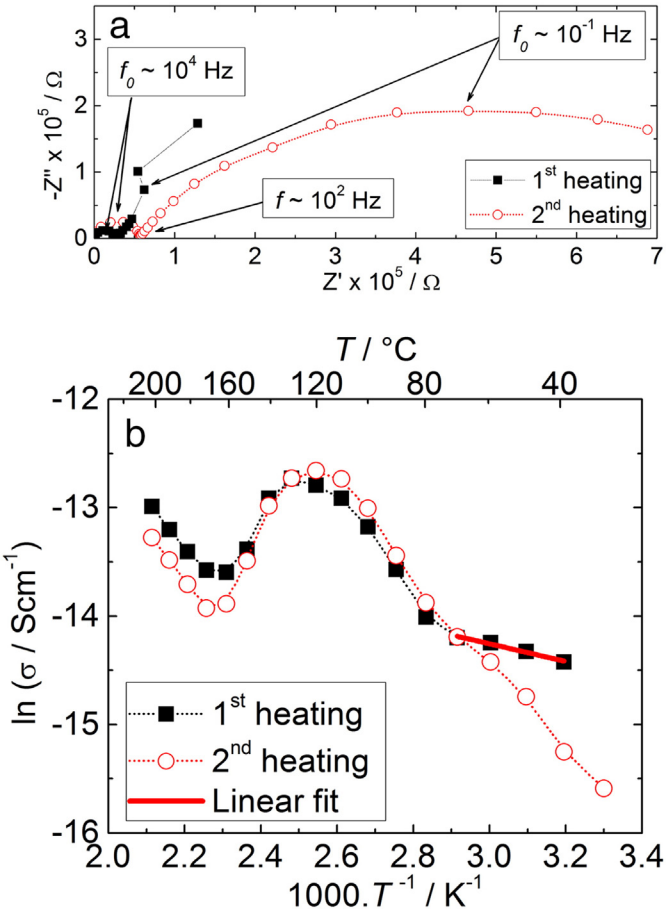

Fig. 3. (a) Nyquist plot of Nafion at two successive heatings under N_2 atmosphere at $T = 50$ °C; and (b) Arrhenius plots for Nafion 115 conductivity (obtained at $f \sim 10^2$ Hz, i.e., the low frequency limit of the first semicircle) at two successive heatings under N_2 atmosphere at $T = 50$ °C.

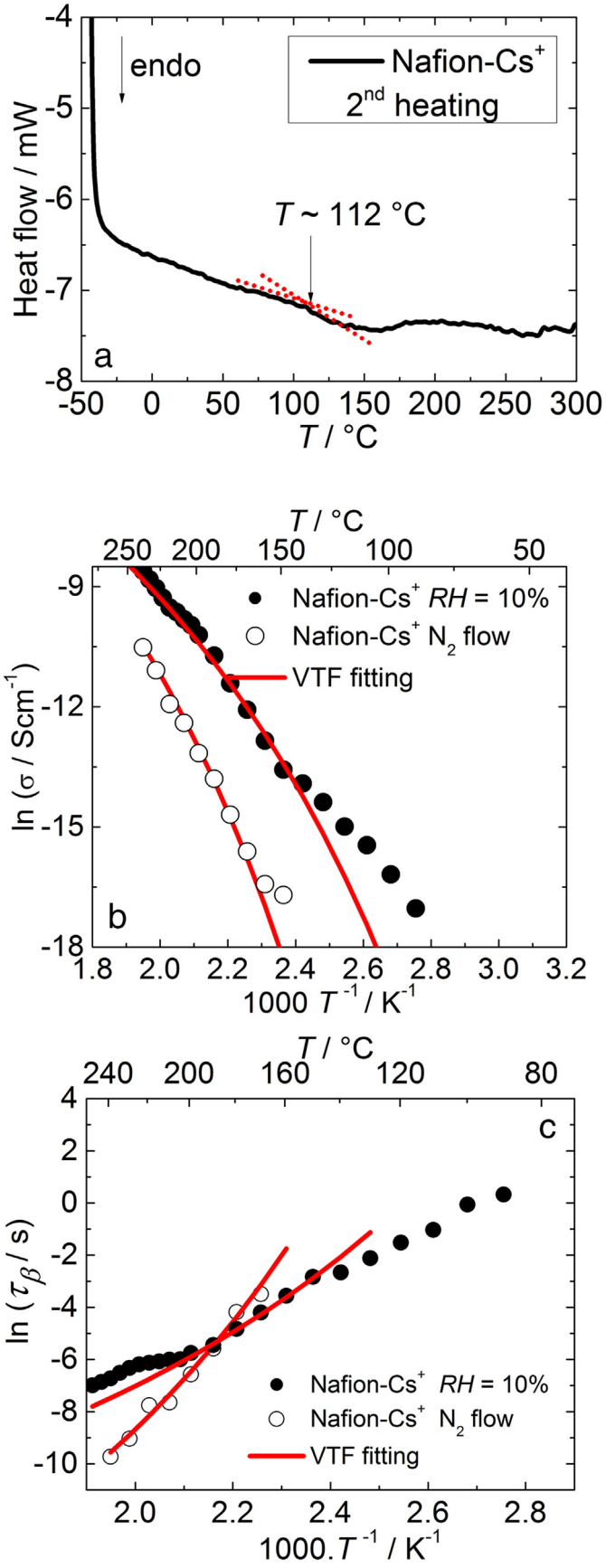

Cs^+: as the effects of α-relaxation are more pronounced at high temperature range ($T > 240$ °C), the proton conductivity is only modulated by the glass transition temperature in a wide $T \sim 110$–240 °C range. Thus, it is possible to probe the glass transition effect on the proton conductivity separately, a condition that is not possible in the acid form of the ionomer. The proton conductivity shown in Fig. 4b clearly shows VTF temperature dependence at $T > 140$ °C reflecting the coupling between the charge transport and the chain motion. The calculated activation energies for the cesium conduction at $RH = 10\%$ and under N_2 flow are, respectively, ~0.20 eV and ~0.25 eV, indicating that the higher flexibility of the polymer chains due to the plasticizing effect of water and the higher degree of solvation of the cesium charges contributed to decrease the activation energy and to increase the cesium conductivity with increasing the *RH* to 10%. Such low conductivity and high activation energy values (Fig. 4b) are characteristic of an ion transport mechanism via vehicular diffusion [21,23]. According to these results, the VTF dependence of ion conductivity can be predominantly attributed to the modulation of the ion conductivity by glass transition of the ionomer matrix.

Fig. 4c shows that the temperature dependence of β-relaxation follows the VTF law, in agreement with previous report [8,17]. The VTF temperature dependence is observed for Nafion-Cs^+ measured at $RH = 10\%$ and ~0% (under N_2 flow). However, the fitted parameters indicate that the glass transition of the sample measured at $RH \sim 10\%$ is lower than the one measured under N_2 flow. The Vogel temperatures used for both *RH* are, respectively, −23 °C and +7 °C. The Vogel temperature is usually 100 K lower than the empirically measured T_g [8]. Therefore, T_0 of the cesium conductivity measured under N_2 suggests a T_g of 107 °C for Nafion-Cs^+, which is in agreement with the values estimated by DSC (Fig. 4a). The lower T_0 of the sample measured at $RH = 10\%$ indicates that the increase of hydration decreases the polymer T_g, possibly due to a plasticization effect.

3.3. Relationship between proton conductivity and relaxation dynamics for hydrated Nafion

The study of nearly dry samples, or containing coordinated water molecules, is simplified as the proton transport is mostly coupled to the motion of Nafion chains. At high *RH*, the protonic charges are expected to be more dissociated from ionic groups and the proton conductivity less dependent on the relaxation dynamics. Therefore, in order to determine how the dynamics of chain motion affects the ion transport in hydrated Nafion, the proton conductivity was studied as a function of temperature at $RH = 100\%$ in a frequency range that coincides with the α and β-relaxation frequencies.

The *ac* conductivity of Nafion was studied in a broad frequency range to evaluate the role played by the α-transition on the temperature dependence of the proton conductivity of hydrated samples [33]. Fig. 5 shows the real component of the proton conductivity as a function of frequency for Nafion-H^+ at $T = 80$ °C and at $RH = 100\%$.

Fig. 5a shows the Nyquist plot of Nafion membrane at $T \sim 80$ °C and $RH = 100\%$, where the frequencies for the *ac* conductivity were obtained. The Nyquist plot displays two superposed semicircles in the ~10^6–10^{-3} Hz *f*-range. The high and low frequency limits of the Nyquist plot approach the real axis ($Z'' \to 0$) at $Z' \sim 0.3\ \Omega$ and $Z' \sim 50\ k\Omega$, respectively, evidencing the two frequency independent processes at $f \sim 10^6$ Hz and $f \sim 10^{-3}$ Hz [8].

The *ac* conductivity of hydrated Nafion allows the separation in the frequency domain of both α relaxation ($f \sim 10^{-1}$ Hz) and glass transition on the conductivity. It is worth noting that in accordance with the conductivity theory for amorphous conductors, the *ac* proton conductivity

Fig. 4. Relation between the glass transition as probed by DSC (a); the high-frequency cesium conductivity (b) of Nafion-Cs^+ at $RH = 10\%$ and at RH ~0% (N_2 flow); and (c) the temperature dependence of the β-relaxation of Nafion-Cs^+ at $RH = 10\%$ and at RH ~0% (N_2 flow).

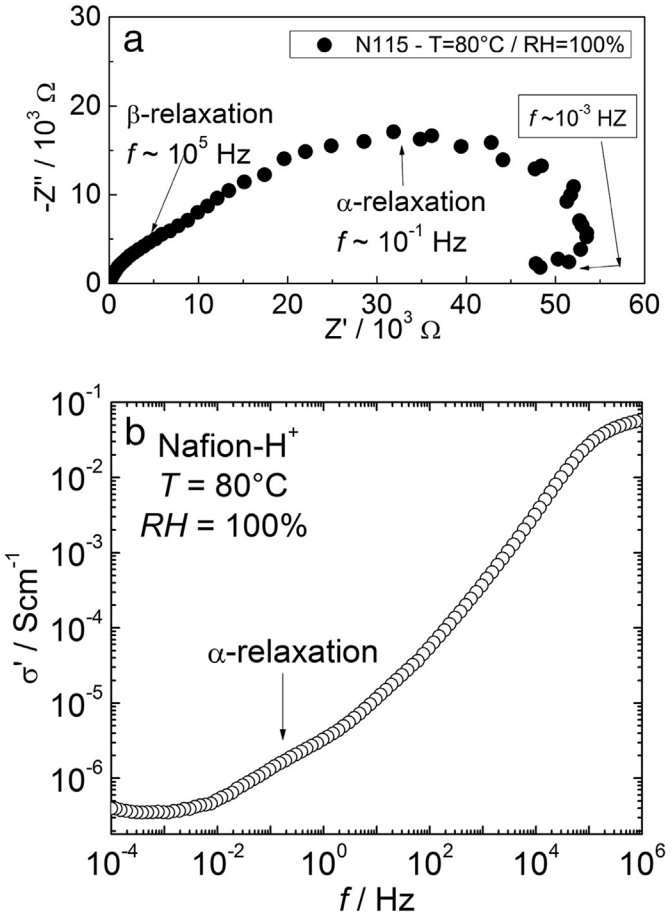

Fig. 5. (a) Impedance spectra of Nafion 115 at $T = 80$ °C and at $RH = 100\%$. Relaxation frequencies of ~10^5 Hz and ~10^{-2} Hz for β and α-relaxations, respectively are indicated; (b) Real component of conductivity as a function of frequency for Nafion 115 at 80 °C and $RH = 100\%$.

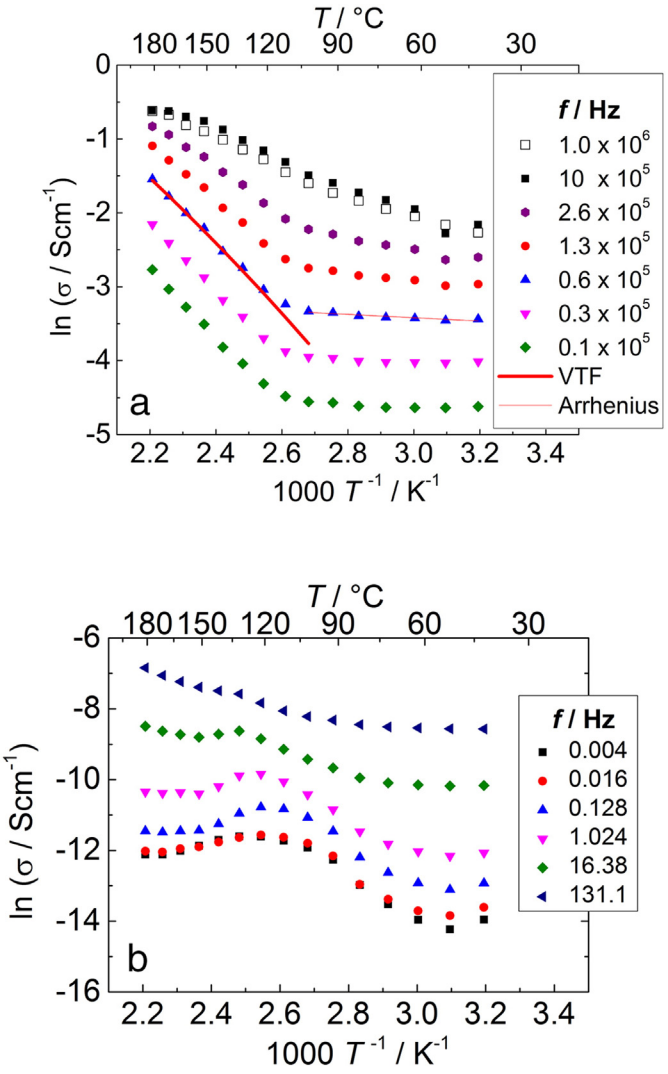

Fig. 6. (a) Arrhenius plot for hydrated N115 proton conductivity at high frequencies ($f > 10^4$ Hz) at $RH = 100\%$; (b) Arrhenius plot for N115 proton conductivity at low frequencies ($f < 10^2$ Hz) at $RH = 100\%$.

is associated with the motion of protonic charges coordinated to charge-compensating site in the polymer chains [34,35]. This feature evidences a close relation between the charge transport and the dynamics of chain motion, which indicates that the proton conductivity of Nafion can be influenced by both the glass transition and the α-relaxation. In Fig. 5b, the DS spectrum at $T = 80$ °C and at $RH = 100\%$ is characterized by a linear decrease with decreasing frequency and a deviation from a linear dependence occurring at $f \sim 10^{-1}$ Hz, which is assigned to dispersions derived from bulk processes [33]. In such frequency range, this dispersion is coincident with the ones observed for α-relaxation ($f \sim 10^{-1}$ Hz) [8,11].

The *ac* conductivity data were measured at several temperatures and plotted by selecting frequencies close to both the α-relaxation frequency (in the low frequency range, $f < 10^2$ Hz) and in the high frequency end of the diagrams ($f > 10^4$ Hz). Such a frequency separation of *ac* conductivity is useful to evaluate the correlation between the proton transport and α-transition in hydrated samples. The temperature dependence of the *ac* proton conductivity at $RH = 100\%$ for N115 is shown in Fig. 6.

It can be observed in Fig. 6a and b that the proton conductivity of hydrated Nafion displays markedly distinct temperature dependences in different frequency ranges. In the high-frequency range ($f > 10^4$ Hz) shown in Fig. 6a, the temperature dependence of proton conductivity is similar to the one commonly observed in amorphous ionic conductors [34,35], in which two regimes can be separated: [15,34] at high T (>90 °C) and the conductivity follows the VTF, whereas at low T (<90 °C), it is dominated by an Arrhenius-like behavior [15,34]. Usually, the Arrhenius-like conductivity at $T < 90$ °C is characterized by the partial dissociation of ionic pairs and the ionic migration between the ionic groups distributed along the polymer backbone [34]. The high conductivity of the polymer at $T > 90$ °C, described by the VTF mechanism, is linked to the ionic migration under the cooperative motion of polymer chains, which exhibit high mobility at $T > T_g$ [34]. Such a behavior suggests that for the hydrated samples at frequencies much higher than the α-transition ($f_\alpha < 10^{-1}$ Hz), the temperature dependence of the proton conductivity is affected by the glass transition of the ionomer [8,17]. The Arrhenius portion of the curve at low temperatures ($T < 90$ °C) is usually attributed to contributions to the conductivity due to extrinsic effects, such as the proton conductivity in the aqueous media, while at high temperatures ($T > 90$ °C) the major contribution to the conductivity is due to intrinsic effects, i.e., the conductivity along the polymer structure [34].

The conductivity curve at $f \sim 0.6 \times 10^5$ Hz (Fig. 6a) was fitted at $T > 90$ °C with the VTF equation. The apparent activation energy in this range is $E_{al} \sim 0.17$ eV. The T_g of acid Nafion cannot be easily obtained since the DSC curves do not clearly exhibit the endothermic inflexion due to the increase of the heat capacity [8,19]. However, previous reports showed by DS measurements that the T_g of acid Nafion is ~−20 °C at RH ~0% [8]. The fitted Vogel temperature for the measurements at $RH = 100\%$, $T_0 = -138$ °C, corresponds to a

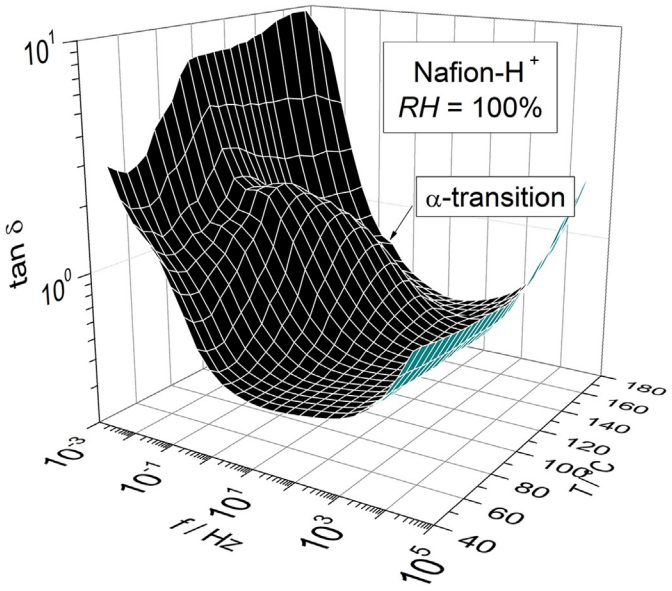

Fig. 7. Dissipation factor curve (tan δ) of Nafion 115 as a function of frequency and temperature at $RH = 100\%$.

$T_g \sim -38$ °C, a value lower than that obtained at $RH \sim 0\%$, which could be a result of T_g reduction due to the presence of water.

It is interesting to note that at a lower frequency range ($10^{-3} < f < 10^{2}$ Hz) the proton conductivity displays a markedly different behavior, as shown in Fig. 6b. This feature is in perfect agreement with the conductivity spectrum shown in Fig. 5 in which the proton conductivity displayed a dependence on the α-relaxation in the $10^{-3} < f < 10^{1}$ Hz range, indicating that the change of the conductivity behavior is due to the coupling between the charge transport with the α-relaxation. Another feature supporting this interpretation is the maximum observed at $T \sim 120$ °C and the general behavior that closely resembles the temperature dependence of Nafion free from uncoordinated water molecules (Fig. 3). Such a remarkable feature indicates that the DS measurements on hydrated samples at low frequencies revealed a similar mechanism of the proton transport of samples measured at $RH \sim 0\%$ (Fig. 3). Therefore, the low-frequency range suggests a correlation between the conductivity and the dynamics of α-relaxation, which occurs at $f \sim 10^{-3}$–10^{2} Hz in hydrated samples.

Fig. 7 shows the dissipation factor curve of Nafion-H^+ as a function of frequency and temperature at $RH = 100\%$. The α-transition peak is observed at $T \sim 120$ °C, in perfect agreement with the conductivity behavior (Fig. 6b) indicating a coupling between the α-relaxation and the transport mechanism at low f.

The electrical and thermomechanical analyzes of Nafion contributed to separate the contributions to the ion transport arising from water content and structural dynamics of the ionomer matrix. The study of the relaxation dynamics on the proton conductivity of Nafion is useful to better understand the performance of such ionomers when used as electrolytes in high-T polymer electrolyte fuel cells. The correspondence between the α-relaxation observed by thermomechanical analyzes and dielectric spectroscopy allowed determining differences in the proton conduction behavior of the samples conditioned both at $RH \sim 0\%$ and 100%. The combination of the proton conductivity studies in both the cesium and proton forms, measured at different hydration states, allowed identifying a noteworthy result: the proton conductivity of water-saturated samples exhibits the coordination of the ion transport with the segmental motion of Nafion main and side chains. Such result is counterintuitive since the dissociation of protons from the polymer chains to the aqueous media would result in an ionic transport less dependent from the polymer chains dynamics. This finding is in agreement with previous SAXS modeling that indicated that the protonic charges may not be fully dissociated from the polymer chains [9,36], thereby the proton conductivity displays a dependence on the polymer dynamics.

4. Conclusions

Conductivity measurements of Nafion in the protonic and cesium forms were performed in a broad range of temperature and frequency. Such experiments revealed interesting features of the proton conductivity of Nafion. The impedance spectroscopy study of Nafion membranes under nitrogen flow, in which the protonic charges are mostly coordinated to the polymer chains, indicated a correlation between the proton conductivity and the α-relaxation. Similar features were observed for the cesium conductivity of Nafion samples conditioned at $RH \sim 0\%$. Due to the higher glass transition temperature of the cesium-neutralized Nafion, the ion transport was mostly coupled to the glass transition of the ionomer. These measurements shed some light into the mechanisms of proton conduction in hydrated samples. The conductivity study of hydrated samples evidenced that the proton transport possesses two markedly distinct regimes: one at higher frequencies ($f > 10^{4}$ Hz) and another at low frequencies ($f \sim 10^{-1}$ Hz), close to the α-relaxation frequency. The high-frequency conductivity followed the VTF law and was attributed to the cooperative motion of the protonic charges and the main chains of Nafion at $T > T_g$. The low-frequency conductivity was assigned to the modulation of the transport of protons by the α-relaxation, similarly to the conductivity of samples at $RH \sim 0\%$.

Acknowledgment

Thanks are due to the Brazilian funding agencies (CAPES, CNPq - 311803/2015-6, FAPESP 2013/50151-5, 2014/09087-4 and 2014/50279-4), to LNLS and to CNEN. FCF is a CNPq fellow. Consejo Nacional de Investigaciones Científicas y Técnicas (CONICET) and the Secretaria de Ciencia y Técnica (SeCyT) of the Universidad Nacional de Córdoba (UNC), Argentina, are acknowledge for financial supports.

References

[1] G. Alberti, M. Casciola, L. Massinelli, B. Bauer, J. Membr. Sci. 185 (2001) 73.
[2] K.D. Kreuer, M. Schuster, B. Obliers, O. Diat, U. Traub, A. Fuchs, U. Klock, S.J. Paddison, J. Maier, J. Power Sources 178 (2008) 499.
[3] M. Fumagalli, S. Lyonnard, G. Prajapati, Q. Berrod, L. Porcar, A. Guillermo, G. Gebel, J. Phys. Chem. B 119 (2015) 7068.
[4] L. Wadsö, P. Jannasch, J. Phys. Chem. B 117 (2013) 8561.

[5] V. Di Noto, E. Negro, J.-Y. Sanchez, C. Iojoiu, J. Am. Chem. Soc. 132 (2010) 2183.
[6] V. Di Noto, M. Piga, G. Pace, E. Negro, S. Lavina, ECS Trans. 16 (2008) 1183.
[7] J.J. Fontanella, M.G. Mclin, M.C. Wintersgill, J. Polym. Sci. B Polym. Phys. 32 (1994) 501.
[8] S.J. Osborn, M.K. Hassan, G.M. Divoux, D.W. Rhoades, K.A. Mauritz, R.B. Moore, Macromolecules 40 (2007) 3886.
[9] J. Li, J.K. Park, R.B. Moore, L.A. Madsen, Nat. Mater. 10 (2011) 507.
[10] M. Casciola, G. Alberti, M. Sganappa, R. Narducci, J. Power Sources 162 (2006) 141.
[11] B.R. Matos, E.I. Santiago, R. Muccillo, I.A. Velasco-Davalos, A. Ruediger, A.C. Tavares, F.C. Fonseca, J. Power Sources 293 (2015) 859.
[12] M. Marechal, J.-L. Souquet, J. Guindet, J.-Y. Sanchez, Electrochem. Commun. 9 (2007) 1023.
[13] R. Yadav, P.S. Fedkiw, J. Electrochem. Soc. 159 (2012) B340.
[14] K. Xu, H. Oh, M.A. Hickner, Q. Wang, Macromolecules 44 (2011) 4605.
[15] B.R. Matos, C.A. Goulart, E.I. Santiago, R. Muccillo, F.C. Fonseca, Appl. Phys. Lett. 109 (2014) 091904.
[16] G.A. Giffin, G.M. Haugen, S.J. Hamrock, V. Di Noto, J. Am. Chem. Soc. 135 (2013) 822.
[17] Z. Lu, G. Polizos, D.D. Macdonald, E. Manias, J. Electrochem. Soc. 155 (2008) B163.
[18] K. Xu, H. Oh, M.A. Hickner, Q. Wang, Macromolecules 44 (2011) 4605.
[19] K.A. Page, K.M. Cable, R.B. Moore, Macromolecules 38 (2005) 6472.
[20] J.-H. Lin, R.H. Colby, J. Polym. Sci. B Polym. Phys. 53 (2015) 1273.
[21] S.C. Yeo, A. Eisenberg, J. Appl. Polym. Sci. 21 (1977) 875.
[22] B.R. Matos, E.I. Santiago, J.F.Q. Rey, C.H. Scuracchio, G.L. Mantovani, L.A. Hirano, F.C. Fonseca, J. Polym. Sci. B Polym. Phys. 53 (2015) 822.
[23] Y.K. Tovbin, N.F. Vasyatkin, Colloids Surf. A Physicochem. Eng. Asp. 158 (1999) 385.
[24] B.R. Matos, M.A. Dresch, E.I. Santiago, M. Linardi, D.Z. de Florio, F.C. Fonseca, J. Electrochem. Soc. 160 (2013) F43.
[25] G. Mao, R.F. Perea, W.S. Howells, D.L. Price, M.-L. Saboungi, Nature 405 (2000) 163.
[26] Y. Kawano, Y. Wang, S.R. Aubuchon, R.A. Palmer, Macromolecules 36 (2003) 1138.
[27] T.A. Zawodzinski Jr., C. Derouin, S. Radzinski, R.J. Sherman, V.T. Smith, T.E. Springer, S. Gottesfeld, J. Electrochem. Soc. 140 (1993) 1041.
[28] M. Ludvigsson, J. Lindgren, J. Tegenfeldt, Electrochim. Acta 45 (2000) 2267.
[29] O. Kwon, S. Wu, D.-M. Zhu, J. Phys. Chem. B 114 (2010) 14989.
[30] I.D. Stefanithis, K.A. Mauritz, Macromolecules 23 (1990) 2397.
[31] B.R. Matos, E.M. Aricó, M. Linardi, A.S. Ferlauto, E.I. Santiago, F.C. Fonseca, J. Therm. Anal. Calorim. 97 (2009) 591.
[32] S.-A. Chen, C.-S. Liao, Macromolecules 26 (1993) 2810.
[33] A. Schönhals, F. Kremer, in: F. Kremer, A. Schönhals (Eds.), Broadband Dielectric Spectroscopy, Springer Verlag, Berlin 2003, p. 59.
[34] S.R. Elliott, Solid State Ionics 70 (1994) 27.
[35] J.C. Dyre, P. Maass, B. Roling, D.L. Sidebottom, Rep. Prog. Phys. 72 (2009) 046501.
[36] K.-D. Kreuer, G. Portale, Adv. Funct. Mater. 23 (2013) 5390.